REPORT DOCUMENTATION PAGE

Form Approved
OMB No. 074-0188

1. AGENCY USE ONLY (Leave blank)	2. REPORT DATE	3. REPORT TYPE AND DATES COVERED
	April 6, 2000	Journal

4. TITLE AND SUBTITLE
An *ab Initio* Study of the Kinetics of the Reactions of Halomethanes with the Hydroxyl Radical. Part 1: CH_2Br_2

5. FUNDING NUMBERS
N/A

6. AUTHOR(S)
Florent Lous, Robert E. Huie, and Michael J. Kurylo

7. PERFORMING ORGANIZATION NAME(S) AND ADDRESS(ES)
Physical and Chemical Properties
Division, National Institute of Standards
and Technology, Gaithersburg, MD
20899

8. PERFORMING ORGANIZATION REPORT NUMBER
N/A

9. SPONSORING / MONITORING AGENCY NAME(S) AND ADDRESS(ES)
SERDP
901 North Stuart St. Suite 303
Arlington, VA 22203

10. SPONSORING / MONITORING AGENCY REPORT NUMBER
N/A

11. SUPPLEMENTARY NOTES

12a. DISTRIBUTION / AVAILABILITY STATEMENT
Approved for public release: distribution is unlimited.

12b. DISTRIBUTION CODE
A

13. ABSTRACT ***(Maximum 200 Words)***

Ab initio calculations using the Moller-Plesset perturbation therory were carried out on the H-atom abstraction reaction from dibromomethane by hydroxyl radical attack. Geometry optimization and vibrational frequency calculations at the MP2 level were performed on all reactants, products and the transition state with both the 6-311G(d,p) and 6-311G(2d,2p) basis sets. Utilizing the geometry parameters optimized at the MP2/6-311G(2d,2p) level of theory, single-point energy calculations were carried out with increasing basis set sizes, from 6-311G(2d, 2p) to 6-311++G(3df, 3pd) and with both the MP2 and MP4SDTQ methods.

Canonical transition state theory was used to predict the rate constants as function of the temperature (240-380 K). For the kinetic parameters of this reaction, reasonable agreement with the experimental values was obtained at the PMP2/6-311G(3df,2p)//MP2/6-311G(2d,2p) level of theory. With the largest basis set, 6-311++G(3df, 3pd), the calculated rate constants are in very good agreement with their experimental counterparts.

14. SUBJECT TERMS
SERDP, SERDP Collection, halomethane, hydroxyl radical, ab initio transition

15. NUMBER OF PAGES
23

16. PRICE CODE
N/A

17. SECURITY CLASSIFICATION OF REPORT	18. SECURITY CLASSIFICATION OF THIS PAGE	19. SECURITY CLASSIFICATION OF ABSTRACT	20. LIMITATION OF ABSTRACT
unclass	unclass	unclass	UL

An *ab Initio* Study of the Kinetics of the Reactions of Halomethanes with the Hydroxyl Radical. Part 1 : CH_2Br_2

Florent LOUIS*, Robert E. HUIE and Michael J. KURYLO

Physical and Chemical Properties Division, National Institute of Standards and Technology, Gaithersburg, Maryland 20899, USA

Abstract

Ab initio calculations using the Møller-Plesset perturbation theory were carried out on the H-atom abstraction reaction from dibromomethane by hydroxyl radical attack. Geometry optimization and vibrational frequency calculations at the MP2 level were performed on all reactants, products and the transition state with both the 6-311G(d,p) and 6-311G(2d,2p) basis sets. Utilizing the geometry parameters optimized at the MP2/6-311G(2d,2p) level of theory, single-point energy calculations were carried out with increasing basis set sizes, from 6-311G(2d,2p) to 6-311++G(3df,3pd) and with both the MP2 and MP4SDTQ methods. Canonical transition state theory was used to predict the rate constants as function of the temperature (240-380 K). For the kinetic parameters of this reaction, reasonable agreement with the experimental values was obtained at the PMP2/6-311G(3df,2p)//MP2/6-311G(2d,2p) level of theory. With the largest basis set, 6-311++G(3df,3pd), the calculated rate constants are in very good agreement with their experimental counterparts.

* Corresponding author, Fax : (301) 975-3672; E-mail: flouis@nist.gov

Introduction

In this paper, we initiate a study of the application of *ab initio* transition state theory to the kinetics of hydrogen-atom abstraction by the hydroxyl radical. The objective of this study is to calculate the enthalpy of the reaction for molecules containing various functional groups, most importantly those containing halogen atoms, and to calculate the rate constants as a function of temperature. From the latter, we calculate Arrhenius A-factors and activation energies. In the present paper, we report the results of our investigation of the reaction:

$$OH + CH_2Br_2 \rightarrow H_2O + CHBr_2 \qquad (1)$$

The initial objective is to establish that level of theory (both method and basis set) which is sufficient to describe the kinetics for this reaction. The computational difficulties in treating the large electronic system associated with bromine make this a serious test of this use of theory and the computational level optimum for this reaction should be adequate for other molecules containing bromine or lighter halogens. Further, bromine is an active agent in fire suppression and inhibition.[1] In the screening for suitability as a fire suppressant, the reactivity of the agent is an important consideration, both with regards to its utility and its environmental acceptability.

There have been some early applications of transition-state theory to the reactions of OH with haloalkanes, making use of thermochemical kinetic tools, which provided estimates of the Arrhenius pre-exponential factors.[2,3] A few *ab initio* studies also have been carried out on the reactions of hydroxyl radicals with halogen-substituted methanes[4-6] or ethanes.[7-11] None of these, however, have been for bromine-substituted methanes. In addition, there have been several *ab initio* studies on the reactions of fluorine and chlorine atoms with halogenated methanes[12-14] and ethanes[15,16] plus one on methyl radical reactions with halomethanes[17]

and a theoretical study of the enthalpies of formation of fluoromethanes.[18] Recently, two *ab initio* studies dealing with the structures, vibrational frequencies, thermodynamic properties, and bond dissociation energies of bromomethanes and bromomethyl radicals were published.[19-21]

Table I summarizes the available results of the experimental studies of the reaction of OH with CH_2Br_2. The rate constant was measured using absolute techniques by Mellouki et al.[22] and Zhang et al.[23] as well as by relative techniques by DeMore[24] and Orlando et al.[25] It was also measured recently in our laboratory at 298 K.[26] With the exception of the relative results of DeMore [24], which have been recalculated with the recommended value for the reference reaction of OH with CH_2Cl_2,[27] the measurements all agree with the value k(298) = 1.2×10^{-13} cm^3 $molecule^{-1}$ s^{-1}.

The kinetic parameters for the reaction of OH with CH_2Br_2 are consistent with a reaction that takes place by hydrogen abstraction. Although recent work has demonstrated that the reaction of the hydroxyl radical with CF_3I proceeds rapidly by I-atom abstraction.[28] The lack of reactivity of CF_3Br towards OH[27] argues against any significant contribution of a bromine abstraction reaction pathway for OH + CH_2Br_2.

Computational Methods[29]

All calculations described below were carried out with the program package Gaussian 94[30] on Cray C90/6256 and SGI Origin 2000 computers. Fully optimized geometry parameters and corresponding vibrational frequencies for the reactants, products and the transition state were computed with the second order Møller-Plesset perturbation theory (UMP2) with the 6-311G(d,p) and 6-311G(2d,2p) basis sets. Spin contamination in the open-shell systems was taken into account by a projection method included in the Gaussian 94

program and is noted in the results as PMPn (n = 2 or 4).[31,32] Vibrational frequencies have been used for the characterization of stationary points, zero-point energy (ZPE) correction and transition state theory (TST) computations of the reaction rate constant. The calculated transition state was confirmed to have one imaginary frequency. All the energies quoted and discussed in the present paper include the zero-point energy correction with unscaled vibrational frequencies.

The optimized geometry parameters at the MP2/6-311G(2d,2p) level of theory were utilized in the calculations of single-point energies. These calculations were carried out at both the MP2 and MP4SDTQ levels of theory and with basis set sizes increasing from 6-311G(2d,2p) to 6-311++G(3df,3pd). Canonical transition state theory and tunneling corrections were used to predict the rate constant over the same range of temperatures as the experimental measurements (240-380 K).[33]

Results and Discussion

1. Geometry Parameters and Vibrational Frequencies

1.1. Geometry parameters

Reactants and products: Table II shows optimized geometry parameters at different levels of theory and also the available experimental data characterizing the structures of these species. All the tested theoretical models produce acceptable parameters for these species.

Transition state: The optimized parameters for the transition state at the two levels of theory are shown in Table III and Figure 1. A comparison of results obtained with the MP2 method and the 6-311G(d,p) and 6-311G(2d,2p) basis sets shows that the parameters calculated for the geometry of the transition state structure are very similar. These results are reflected in the transition state parameter L which is defined as the ratio between the increase

in length of the C-H bond being broken and the elongation of the O-H bond being formed, each with respect to its equilibrium value in the reactant (CH_2Br_2) and the product (H_2O).[12] This parameter characterizes the most important aspect of the geometric structure of the transition state. When the basis set included two d-orbital polarization functions on the heavy atoms (C and Br) and two p-orbital polarization functions on the H atoms, the parameter L changes only slightly. This suggests that the MP2/6-311G(2d,2p) level of theory gives adequate results for the geometry of the transition state. Consequently, these MP2/6-311G(2d,2p) optimized geometry parameters will be used for the single-point energy calculations.

1.2. Vibrational frequencies

The vibrational frequencies, unscaled zero-point energies and internal energy corrections at 298 K for reactants, transition state and products are given in Tables IV and V. For reactants and products, calculated vibrational frequencies values at the MP2/6-311G(d,p) and MP2/6-311G(2d,2p) are about 7% greater than the experimental values. In the transition state, the eigenvector corresponding to the imaginary frequency is primarily a motion of the reactive hydrogen atom being transferred between the C and O centers. The calculated value of the imaginary frequency is about 6% larger at the MP2/6-311G(2d,2p) level of theory than at the MP2/6-311G(d,p) level. This fact was previously observed for the series of H-atom abstraction reactions F + $CHCl_{3-x}F_x$ (x = 0, 1, 2 or 3).[13]

2. Reaction enthalpies and activation energies

The effect of the basis set and the influence of higher-order electron correlation and spin projections on the calculated total energies of the transition state, reactants and products

are shown in Table VI. All the single-point energy calculations were done with the MP2/6-311G(2d,2p) optimized geometry parameters except for the first, which used the MP2/6-311G(d,p) optimized geometry parameters.

In the first step, we calculated single-point energies for reactants, products and transition state at different levels of theory. Corresponding reaction enthalpies ($\Delta_r H$) and activation energies (E_a), taking into account the zero-point energy difference and thermal energy corrections at 298 K (calculated using the vibrational frequencies given in Table IV), are displayed in Table VII (columns 2 and 5).

The two geometry optimization levels of theory give calculated reaction enthalpies that were very close to the literature values based on $\Delta_f H^0$ at 298 K for OH,[34] CH_2Br_2,[35] H_2O,[34] and $CHBr_2$,[36] particularly when the stated uncertainties for CH_2Br_2 (± 9 kJ mol^{-1}) and $CHBr_2$ (± 5 kJ mol^{-1}) are taken into consideration. Adding diffuse functions to the basis set with MP2 method led to calculated reaction enthalpies $\Delta_r H$ outside the experimental uncertainties. With all the other tested theoretical models, a satisfying agreement was obtained between experimental reaction enthalpies and their calculated counterparts.

In order to get a much closer agreement between experimental and *ab initio* values, especially for the basis sets including diffuse functions, reaction enthalpies for reaction (1) were also corrected for the different levels of theory by utilizing the isodesmic reaction

$$CH_3 + CH_2Br_2 \rightarrow CH_4 + CHBr_2 \qquad (2)$$

to calculate D_{298} (H-$CHBr_2$). The direct calculation of this bond dissociation energy from the reaction $CH_2Br_2 \rightarrow H + CHBr_2$ is expected to be systematically in error due to insufficient treatment of electron correlation and incompleteness of the basis sets. The use of an isodesmic reaction, such as reaction (2), provides an indirect method which may lead to a more reliable value of the bond dissociation energy. The specific property of an isodesmic

reaction is that there are the same number and type of bonds on each side of the equation, so that the errors mentioned above are largely canceled in the calculated value of D_{298} (H-$CHBr_2$). The reaction enthalpy for reaction (2) was calculated at the same levels of theory as that for reaction (1). Taking the experimental value of D_{298}(H-CH_3) = 440 kJ mol^{-1},[37] we obtain calculated D_{298} (H-$CHBr_2$) values at the various levels of theory (Table VII, column 3). Then the reaction enthalpy for reaction (1) are determined as $\Delta_r H$ (ISO) = D_{298}(H-$CHBr_2$) - D_{298} (H-OH). Table VII (column 4) contains these new values which can be compared to the direct calculations (column 2) and to their experimental counterparts. The improvement observed is quite significant, especially for the basis sets with diffuse functions.

The activation energy calculated at the PMP2/6-311G(d,p)//MP2/6-311G(d,p) level of theory is about 13-14 kJ mol^{-1} higher than the measured value. Improvement of the basis set to 6-311G(2d,2p) yields a decrease in the value activation energy by 2.9 kJ mol^{-1}. Increasing the basis set size by adding more polarization functions and diffuse functions led to decrease the values of activation energy so that the differences between calculated and experimental activation energies for the OH + CH_2Br_2 reaction become smaller, i.e. 5.0 to 3.5 kJ mol^{-1} respectively for the PMP2/6-311G(3df,2p) and the largest basis set with both MP2 and MP4STDQ methods.

3. Kinetic parameters and tunneling effect

The knowledge of the geometry and vibrational frequencies characterizing the transition state (Tables III and IV) enables us to calculate the corresponding activation entropy (Δ^*S) and the Arrhenius A-factor using conventional transition state theory. Table VIII collects the values of molar entropies calculated at 298 K for reactants and the transition state, the ones of resulting activation entropies and the Arrhenius A-factors calculated at the two

geometry optimization levels. At both the MP2/6-311G(d,p) and MP2/6-311G(2d,2p) levels of theory, good agreement with the calculated and experimental values of the molar entropies were obtained. The electronic contribution of the molar entropy of the hydroxyl radical took into account the multiplicity of the states and the energy gap of 139.7 cm^{-1} between the $^2\Pi_{3/2}$ and $^2\Pi_{1/2}$ levels.[34] The resulting A-factors are in good agreement with experiment.

For the reactions involving a hydrogen-atom transfer, the tunneling effect must be estimated. The great importance of this correction suggests that a preferable approach to obtaining the Arrhenius parameters is through the calculation of the rate constants for the reaction over a range of temperatures, with a subsequent fit of the rate constants to the Arrhenius equation. The rate constants were calculated over the same temperature range as the measured values (i.e. 240 to 380 K) using the canonical transition state theory formalism[33] including the symmetrical Eckart tunneling correction, $\Gamma(T)$[38]

$$k(T)=\Gamma(T)\times\frac{k_b T}{h}\times\frac{Q^{\neq}(T)}{Q_{OH}(T)\,Q_{CH2Br2}(T)}\times\exp\left(-\frac{\Delta E}{k_b T}\right) \qquad (I)$$

where $Q^{\neq}(T)$, $Q_{OH}(T)$ and $Q_{CH2Br2}(T)$ are the total partition functions for the transition state, hydroxyl radical, and dibromomethane at temperature T; ΔE is the activation energy including thermal corrections to the internal energy and zero-point energy; k_b is the Boltzman constant; and h the Planck constant. Calculated tunneling parameters using the symmetrical Eckart's correction are included in the range 4.0 to 10.0 as function of the temperature. At room temperature, their values are about 5.8 to 7.2 depending on the level of theory used.

Symmetrical Eckart tunneling is more appropriate to calculate the tunneling factor than the Wigner's correction.[38] For even better agreement, more sophisticated methods such as the small curvature approximation are necessary.[39] In this case, detailed knowledge of the

reaction path is needed and this method is very time consuming with a large electronic system such as that for the bromine atom.

The results of the calculations of the rate constants at different levels of theory are shown in Figure 2 and a summary of the calculated Arrhenius parameters including the tunneling correction is given in Table IX. Regardless of the level of theory, the calculated Arrhenius A-factors are similar and in reasonable agreement with the experimental value. The calculated values of the activation energy, however, depend strongly on the level of theory. With the largest basis set, 6-311++G(3df,3pd), and with either the MP2 or MP4SDTQ methods, the predicted rate constants are in very good agreement with their experimental counterparts over the whole temperature range. At the PMP2/6-311G(3df,2p)//MP2/6-311G(2d,2p) level of theory, which is significantly less computationally demanding, the calculated rate constants are 47 % lower than the measured values over the temperature range (240-380) K.

Conclusion

Ab initio calculations were performed at different levels of theory for the H-atom abstraction reaction between dibromomethane and hydroxyl radicals. The geometry parameters for reactants, products and transition state were first fully optimized at the MP2/6-311G(d,p) level of theory and then reoptimized with the 6-311G(2d,2p) basis set. The parameter L changed only slightly, suggesting that the MP2/6-311G(2d,2p) level of theory gives adequate results for the geometry of the transition state. Hence it appears that no higher basis set is needed for the optimization of the geometry parameters in subsequent investigations of the reactions of OH with other halomethanes. The calculation of the energetics of the reaction and, subsequently, the kinetic parameters, proved more dependent

on the level of theory, particularly on the nature and extent of the basis set. The best fit to the experimental data was with the 6-311++G(3df,3pd) basis sets, employing either the MP2 or MP4SDTQ methods. A quite reasonable agreement, within a factor of two, was obtained with the far less computationally intensive MP2 method with a 6-311G(3df,2p) basis set. These levels of theory are applied in our subsequent work to a broader range of halocarbon reactions with the hydroxyl radical. The results for reactions involving halomethanes of type CHXYZ (X, Y, Z = H, F, Cl or Br) indicate that the energetics and kinetics are well described with these levels of theory and that the calculated rate constants are in very good agreement with their experimental counterparts.

Acknowledgements

This work was supported by the Upper Atmosphere Research Program of the National Aeronautics and Space Administration and by Next Generation Fire Suppression Technology Program, funded by the Department of Defense Strategic Environmental Research and Development Program under MIPR number W74RDV73243630.

We thank C. Gonzalez (NIST) for providing the program to calculate k and for many fruitful discussions. We are also grateful to D. Burgess (NIST) and V. Orkin for helpful discussions.

Table I : Experimental rate parameters for the reaction $OH + CH_2Br_2 \rightarrow H_2O + CHBr_2$

A ($cm^3.molecule^{-1}.s^{-1}$)	E_a ($kJ\ mol^{-1}$)	T (K)	k (298 K) ($cm^3.molecule^{-1}.s^{-1}$)	Method	Ref.
1.9×10^{-12}	7.0	244-370	$1.1_4 \times 10^{-13}$	FP/LIF[a]	*22*
3.2×10^{-12}	7.5	293-375	1.5×10^{-13}	RR[b]	*24*
		298	1.2×10^{-13}	RR[b]	*25*
1.5×10^{-12}	6.0	288-368	1.3×10^{-13}	DF/RF[c]	*23*
		298	1.2×10^{-13}	FP/RF[d]	*26*

[a] FP/LIF : Flash Photolysis/Laser Induced Fluorescence, [b] RR : Relative Rate, [c] DF/RF : Discharge Flow/Resonance Fluorescence, [d] FP/RF : Flash Photolysis/Resonance Fluorescence

Table II : Optimized geometry parameters for reactants and products involved in H-abstraction reaction of CH_2Br_2 with hydroxyl radicals

	Parameter[a]	MP2 6-311G(d,p)	MP2 6-311G(2d,2p)	Expt
OH	r (OH)	0.967	0.965	*0.971*[b]
CH_2Br_2	r (CH)	1.086	1.078	*1.097*[c]
	r (CBr)	1.929	1.933	*1.925*
	θ (HCH)	111.6	111.9	*110.9*
	θ (BrCH)	107.8	107.9	
	ϕ (BrCHH)	118.2	118.5	
H_2O	r (OH)	0.958	0.957	*0.958*[d]
	θ (HOH)	102.4	103.3	*104.5*
$CHBr_2$	r (CH)	1.082	1.074	
	r (CBr)	1.860	1.861	
	θ (BrCH)	116.0	116.1	
	ϕ (BrCHBr)	148.4	149.2	

[a] Bond lengths are in Angströms, bond angles θ and dihedral angles ϕ are in degrees. Experimental values taken from [b] *ref. 34*, [c] *ref. 40*, [d] *ref. 41*

Table III : Optimized geometry parameters for transition state involved in H-atom abstraction reaction of CH_2Br_2 with hydroxyl radicals

Parameter[a]	MP2 6-311G(d,p)	MP2 6-311G(2d,2p)
r (C-H_R)	**1.192**	**1.188**
r (CH)	1.087	1.078
r ($CBr_{(a)}$)	1.910	1.911
r ($CBr_{(b)}$)	1.917	1.919
r (OH_R)	**1.296**	**1.296**
r (HO)	0.968	0.967
θ (HCH_R)	108.2	108.2
θ ($Br_{(a)}CH_R$)	105.8	106.0
θ ($Br_{(b)}CH_R$)	108.0	107.8
θ (OH_RC)	**166.2**	**165.3**
θ (HOH_R)	97.1	97.2
ϕ ($Br_{(a)}CH_RH$)	117.8	118.1
ϕ ($Br_{(b)}CH_RH$)	-118.3	-118.4
ϕ (OH_RCH)	48.5	51.9
ϕ (HOH_RC)	50.7	51.5
L[b]	0.314	0.324

[a] Bond lengths are in Angströms, bond angles θ and dihedral angles ϕ are in degrees ; the hydrogen atom involved in H-atom abstraction is noted H_R, (a) refers to the in-plane bromine and (b) to the out-of-plane bromine

[b] the parameter L is the ratio between the elongation value of the C-H bond and the elongation of the O-H bond : $L = \delta r(CH)/\delta r(OH)$

Table IV : Calculated[1-2] vibrational frequencies (cm^{-1}) for reactants, transition state and products involved in H-atom abstraction reaction of CH_2Br_2 with hydroxyl radicals

Species	Vibrational frequencies (cm^{-1})
OH	[1] 3853
	[2] 3833
	3735[a]
CH_2Br_2	[1] 178, 604, 692, ,835, 1150, 1265, 1459, 3169, 3254
	[2] 175, 590, 672, 833, 1141, 1239, 1458, 3183, 3270
	169, 588, 653, 812, 1095, 1195, 1382, 3009, 3073[b]
TS	[1] 2075i, 70, 102, 155, 183, 473, 651, 713, 805, 959, 1210, 1319, 1405, 3211, 3840
	[2] 2200i, 76, 109, 156, 182, 463, 640, 698, 803, 957, 1191, 1307, 1395, 3225, 3811
H_2O	[1] 1667, 3905, 4013
	[2] 1685, 3875, 3989
	1595, 3657, 3756[b]
$CHBr_2$	[1] 193, 492, 653, 805, 1241, 3267
	[2] 189, 486, 644, 790, 1214, 3279
	633, 778, 1164[c]

[1] MP2/6-311G(d,p) and [2] MP2/6-311G(2d,2p)

The experimental values of the vibrational frequencies are in italics. These values are taken from [a] *ref. 34* [b] *ref. 42* [c] *ref. 43*

Table V : Calculated zero-point Energy and thermal energy corrections at 298 K for reactants, transition state and products involved in H-atom abstraction reaction of CH_2Br_2 with hydroxyl radicals

	Zero-point Energy[a]	Thermal Energy[a]
OH	23.1[b] / 22.9[c]	6.2
CH_2Br_2	75.4/75.1	10.1
H_2O	57.3/57.1	7.5
$CHBr_2$	39.8/39.5	10.2
TS	90.3/89.8	16.4

[a] Units are kJ mol^{-1}; geometry optimization calculations at [b]MP2/6-311G(d,p) and [c]MP2/6-311G(2d,2p) levels of theory

Table VI : Total energies (Hartree) for species involved in the OH + CH_2Br_2 reaction

Level of theory[a]	OH	CH_2Br_2	H_2O	$CHBr_2$	TS
PMP2/6-311G(d,p)	-75.5743877	-5184.1718628	-76.2639719	-5183.5137735	-5259.7364004
PMP2/6-311G(2d,2p)	-75.5924012	-5184.1863148	-76.2864796	-5183.5249410	-5259.7699038
PMP2/6-311G(2df,2p)	-75.6098490	-5184.2605878	-76.3053759	-5183.5997077	-5259.8629601
PMP2/6-311G(3df,2p)	-75.6129582	-5184.2867716	-76.3088420	-5183.6260478	-5259.8929791
PMP4SDTQ/6-311G(3df,2p)	-75.6304870	-5184.3466716	-76.3235883	-5183.6836430	-5259.9700200
PMP2/6-311++G(3df,2p)	-75.6196701	-5184.2883243	-76.3184016	-5183.6277812	-5259.9002291
PMP4SDTQ/6-311++G(3df,2p)	-75.6372940	-5184.3483066	-76.3329564	-5183.6855040	-5259.9776740
PMP2/6-311++G(3df,3pd)	-75.6227493	-5184.2925559	-76.3242589	-5183.6299602	-5259.9090990
PMP4SDTQ/6-311++G(3df,3pd)	-75.6402720	-5184.3521435	-76.3386595	-5183.6874970	-5259.9862380

[a] All the geometry optimization calculations were done with the MP2/6-311G(2d,2p) except the first with MP2/6-311G(d,p)

Table VII : Reaction enthalpies $\Delta_r H$, bond strengths $D_{298}(H\text{-}CHBr_2)$, reactions enthalpies $\Delta_r H$ (ISO) calculated using an isodesmic reaction and activation energies calculated at 298 K for the reaction $OH + CH_2Br_2 \rightarrow H_2O + CHBr_2$ at various levels of theory

Level of theory[a]	$\Delta_r H$ [b,d]	$D_{298}(H\text{-}CHBr_2)$[d]	$\Delta_r H$ (ISO)[b,d]	Activation energy[c,d]
PMP2/6-311G(d,p)	-82.7	412.7	-86.1	20.3
PMP2/6-311G(2d,2p)	-86.0	415.1	-83.7	17.4
PMP2/6-311G(2df,2p)	-91.1	412.1	-86.7	13.9
PMP2/6-311G(3df,2p)	-92.4	411.3	-87.5	12.0
PMP4SDTQ/6-311G(3df,2p)	-79.1	409.3	-89.5	13.0
PMP2/6-311++G(3df,2p)	-100.4	413.3	-85.5	14.6
PMP4SDTQ/6-311++G(3df,2p)	-86.4	411.3	-87.5	15.1
PMP2/6-311++G(3df,3pd)	-102.3	414.9	-83.9	10.6
PMP4SDTQ/6-311++G(3df,3pd)	-88.7	413.1	-85.7	10.5
Experimental	*-81.6* [e]	*417.1* [e]	*-81.6* [e]	*7.0*[f]

[a] All the geometry optimization calculations were done with the MP2/6-311G(2d,2p) except the first with MP2/6-311G(d,p), [b] including the sum of thermal energies (ΔZPE + thermal energy corrections), [c] including the sum of thermal energies (ΔZPE + thermal energy corrections + RT), [d] in $kJ.mol^{-1}$, [e] *see text*, [f] from *ref.* [22]

Table VIII : Entropies of reactants (S), transition state ($S^{\neq}$) and activation entropy ($\Delta^{\neq}S$) and preexponential factor calculated at 298 K at different levels of theory

		S	$S^{\neq}$	$\Delta^{\neq}S$	$A \times 10^{12}$
		J mol^{-1} K^{-1}	J mol^{-1} K^{-1}	J mol^{-1} K^{-1}	cm^3 $molecule^{-1}$ s^{-1}
MP2/6-311G(d,p)	**OH**	185.8			
MP2/6-311G(2d,2p)		185.8			
		(183.7)[a]			
MP2/6-311G(d,p)	**CH_2Br_2**	298.3	361.1	-123.0	1.4
MP2/6-311G(2d,2p)		298.7	360.2	-124.3	1.2
		(293.3)[b]			

[a] From ref. 34

[b] From ref. 40

Table IX : Summary of Arrhenius parameters calculated at different levels of theory including the tunneling correction

Method	Basis Set	k_{calc} [a]	Γ (298 K)	Ea (kJ mol^{-1})	A[a] × 10^{12}	Γ × k_{calc} [a] (298 K)	Γ × k_{calc} /k_{exp} (298 K) [b]
MP2	6-311G(d,p)	3.9×10^{-16}	5.8	16.3	1.6	2.2×10^{-15}	0.02
MP2	6-311G(2d,2p)	1.1×10^{-15}	6.5	13.2	1.4	6.8×10^{-15}	0.06
MP2	6-311G(2df,2p)	4.5×10^{-15}	6.7	9.7	1.5	3.0×10^{-14}	0.25
MP2	6-311G(3df,2p)	9.6×10^{-15}	6.9	7.8	1.5	6.4×10^{-14}	0.53
MP4SDTQ	6-311G(3df,2p)	6.4×10^{-15}	6.8	8.8	1.5	4.3×10^{-14}	0.36
MP2	6-311++G(3df,2p)	3.3×10^{-15}	6.7	10.4	1.5	2.3×10^{-14}	0.19
MP4SDTQ	6-311++G(3df,2p)	2.8×10^{-15}	6.6	10.9	1.5	1.8×10^{-14}	0.15
MP2	6-311++G(3df,3pd)	1.6×10^{-14}	7.1	6.6	1.6	1.1×10^{-13}	0.92
MP4SDTQ	6-311++G(3df,3pd)	1.8×10^{-14}	7.2	6.2	1.6	1.3×10^{-13}	1.08

[a] Units are cm^3.molecule^{-1}.s^{-1}, [b] k_{exp} (298 K) = 1.2×10^{-13} cm^3.molecule^{-1}.s^{-1} from *ref. 27.*

References

1) Noto, T.; Babushok, V.; Burgess, D. R.; Hamins, A.; Tsang, W.; Miziolek, A. *Twenty-Sixth Symp. (Int.) Comb.* **1996**, 1377.

2) Jeong, K. M.; Kaufman, F. *J. Phys. Chem.* **1982**, *86*, 1816.

3) Cohen, N.; Benson, S. W. *J. Phys. Chem.* **1987**, *91*, 162.

4) Bottoni, A.; Poggi, G.; Emmi, S. S. *J. Molec. Struc. (Theochem)* **1993**, *279*, 299.

5) Fu, Y.; Lewis-Bevan, W.; Tyrell, J. *J. Phys. Chem.* **1995**, *99*, 630.

6) Schwartz, M.; Marshall, P.; Berry, R. J.; Ehlers, C. J.; Petersson, G. A. *J. Phys. Chem. A* **1998**, *102*, 10074.

7) Martell, J. M.; Boyd, R. J. *J. Phys. Chem.* **1995**, *99*, 13402.

8) Sekusak, S.; Gusten, H.; Sabljic, A. *J. Chem. Phys.* **1995**, *102*, 7504.

9) Sekusak, S.; Gusten, H.; Sabljic, A. *J. Phys. Chem.* **1996**, *100*, 6212.

10) Sekusak, S.; Sabljic, A. *Chem. Phys. Lett.* **1997**, *272*, 353.

11) Sekusak, S.; Liedl, K. R.; Rode, B. M.; Sabljic, A. *J. Phys. Chem. A* **1997**, *101*, 4245.

12) Rayez, M.-T.; Rayez, J.-C.; Sawerysyn, J.-P. *J. Phys. Chem.* **1994**, *98*, 11342.

13) Louis, F. ; University of Lille: Lille, France, 1997.

14) Louis, F.; Rayez, M.-T.; Rayez, J.-C.; Sawerysyn, J.-P. *Phys. Chem. Chem. Phys.* **1999**, *3*, 383.

15) Talhaoui, A.; Louis, F.; Devolder, P.; Meriaux, B.; Sawerysyn, J.-P.; Rayez, M.-T.; Rayez, J.-C. *J. Phys. Chem.* **1996**, *100*, 13531.

16) Louis, F.; Talhaoui, A.; Sawerysyn, J.-P.; Rayez, M.-T.; Rayez, J.-C. *J. Phys. Chem. A* **1997**, *101*, 8503.

17) Bernardi, F.; Bottoni, A. *J. Phys. Chem. A* **1997**, *101*, 1912.

18) Berry, R. J.; Burgess, D. R. F.; Nyden, M. R.; Zachariah, M. R. *J. Phys. Chem.* **1995**, *99*, 17145.

19) Paddison, S. J.; Tschuikow-Roux, E. *J. Phys. Chem.* **1998**, *102*, 6191.

20) Paddison, S. J.; Tschuikow-Roux, E. *Int. J. Thermophys.* **1998**, *19*, 719.

21) Kambanis, K. G.; Lazarou, Y. G.; Papagiannakopoulos, P. *J. Phys. Chem. A* **1997**, *101*, 8496.

22) Mellouki, A.; Talukdar, R. K.; Schmoltner, A. M.; Gierczak, T.; Mills, M. J.; Solomon, S.; A.R. Ravishankara *Geophys. Res. Lett* **1992**, *19*, 2059.

23) Zhang, D. Q.; Zhong, J. X.; Qiu, L. X. *J. Atmos. Chem.* **1997**, *27*, 209.

24) DeMore, W. B. *J. Phys. Chem* **1996**, *100*, 5813.

25) Orlando, J. J.; Tyndall, G. S.; Wallington, T. J.; Dill, M. *Int. J. Chem. Kinet.* **1996**, *28*, 433.

26) Orkin, V.; Huie, R. E.; Kurylo, M. J. *Unpublished work* .

27) DeMore, W. B.; Sander, S. P.; Golden, D. M.; Hampson, R. F.; Kurylo, M. J.; Howard, C. J.; Ravishankara, A. R.; Kolb, C. E.; Molina, M. J. *JPL Publication 97-4* **1997**, *Evaluation 12*.

28) Berry, R. J.; Yuan, J.; Misra, A.; Marshall, P. *J. Phys. Chem. A* **1998**, *102*, 5182.

29) The identification of commercial equipment or materials does not imply recognition or endorsement by the National Institute of Standards and Technology, nor does it imply that the material or equipment identified are necessarily the best available for the purpose.

30) Frisch, M. J.; Trucks, G. W.; Schlegel, H. B.; Gill, P. M. W.; Johnson, B. G.; Robb, M. A.; Cheeseman, J. R.; Keith, T.; Petersson, G. A.; Montgomery, J. A.; Raghavachari, K.; Al-Laham, M. A.; Zakrzewski, V. G.; Ortiz, J. V.; Foresman, J. B.; Cioslowski, J.; Stefanov, B. B.; Nanayakkara, A.; M. Challacombe; Peng, C. Y.; Ayala, P. Y.; Chen, W.; Wong, M. W.;

Andres, J. L.; Replogle, E. S.; Gomperts, R.; Martin, R. L.; Fox, D. J.; Binkley, J. S.; Defrees, D. J.; Baker, J.; Stewart, J. P.; Head-Gordon, M.; Gonzalez, C.; Pople, J. A. *GAUSSIAN 94*; Revision D.4 ed.; Frisch, M. J.; Trucks, G. W.; Schlegel, H. B.; Gill, P. M. W.; Johnson, B. G.; Robb, M. A.; Cheeseman, J. R.; Keith, T.; Petersson, G. A.; Montgomery, J. A.; Raghavachari, K.; Al-Laham, M. A.; Zakrzewski, V. G.; Ortiz, J. V.; Foresman, J. B.; Cioslowski, J.; Stefanov, B. B.; Nanayakkara, A.; M. Challacombe; Peng, C. Y.; Ayala, P. Y.; Chen, W.; Wong, M. W.; Andres, J. L.; Replogle, E. S.; Gomperts, R.; Martin, R. L.; Fox, D. J.; Binkley, J. S.; Defrees, D. J.; Baker, J.; Stewart, J. P.; Head-Gordon, M.; Gonzalez, C.; Pople, J. A., Ed.; Gaussian, Inc: Pittsburgh PA, 1995.

31) Sosa, C.; Schlegel, H. B. *Int. J. Quantum Chem.* **1986**, *29*, 1001.

32) Sosa, C.; Schlegel, H. B. *Int. J. Qunatum Chem.* **1987**, *30*, 155.

33) Rate constants calculated with the turbo-rate module in the turbo-opt geometry optimization package, developed by C. Gonzalez, National Institute of Standards and Technology, Gaithersburg, MD .

34) Chase, M. W. *J. Phys. Chem. Ref. Data* **1998**, *Monograph 9*.

35) Bickerton, J.; Minas da Piedade, M. E.; Pilcher, G. *J. Chem. Thermo.* **1984**, *16*, 661.

36) Tschuikow-Roux, E.; Paddison, S. *Int. J. Chem. Kinet.* **1987**, *19*, 15.

37) Tsang, W. *Heats of formation of organic free radicals by kinetic methods*; Tsang, W., Ed.; Blackie Academic & Professional: London, 1996, pp 22.

38) Johnston, H. S. *Gas Phase Reaction Rate Theory*; The Roland Press Company: New York, 1966.

39) Skodje, R. T.; Truhlar, D. G.; Garet, B. C. *J. Chem. Phys.* **1982**, *77*, 5955.

40) Kudchadker, S. A.; Kudchadker, A. P. *J. Phys. Chem. Ref. Data* **1975**, *4*, 457.

41) Lide, D. R. *Handbook of Chemistry and Physics*; Lide, D. R., Ed.; CRC Press: Boca raton, FL, 1990.

42) Shimanouchi, T. *NSRDS-NBS* **1972**, *39*.

43) Jacox, M. E. *Vibrational and Electronic Energy Levels of Polyatomic Transient Molecules*; Jacox, M. E., Ed.; National Institute of Standards and Technology, 1998; Vol. 69, pp 945.

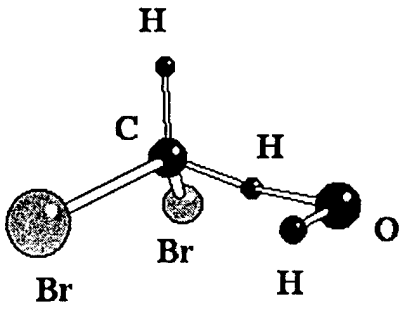

Figure 1 : MP2/6-311G(2d,2p) optimized geometry for the transition state involved in the OH + CH_2Br_2 reaction

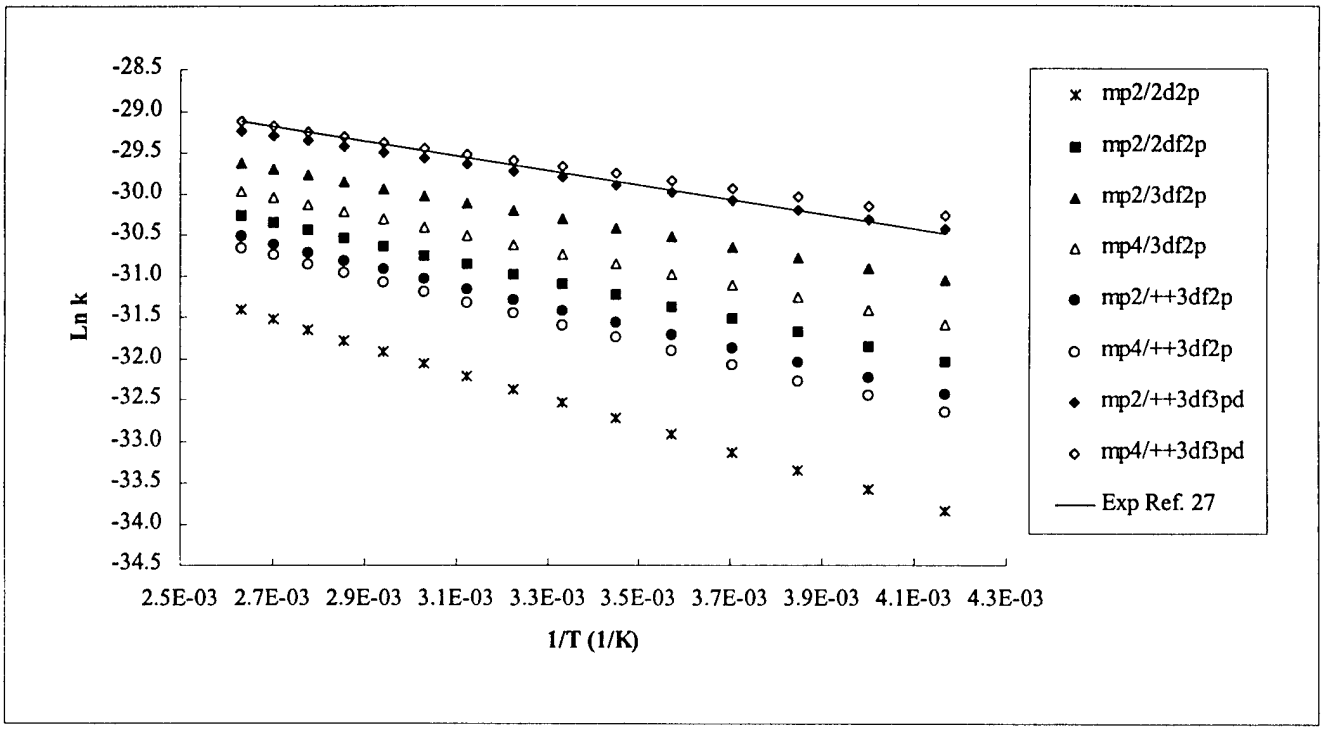

Figure 2 : Arrhenius plots for OH + CH_2Br_2 → H_2O + $CHBr_2$ for the different levels of theory used in this study. The notations mp2/2d2p to mp4/++3df3pd in the legend mean PMP2/6-311G(2d,2p) to PMP4SDTQ/6-311++G(3df,3pd).